The estimation of lower refractivity uncertainty from radar sea clutter using the Bayesian–MCMC method*

Sheng Zheng(盛 峥)†

College of Meteorology and Oceangraphy, PLA University of Science and Technology, Nanjing 211101, *China*

(Received 7 May 2012; revised manuscript received 4 July 2012)

The estimation of lower atmospheric refractivity from radar sea clutter (RFC) is a complicated nonlinear optimization problem. This paper deals with the RFC problem in a Bayesian framework. It uses the unbiased Markov Chain Monte Carlo (MCMC) sampling technique, which can provide accurate posterior probability distributions of the estimated refractivity parameters by using an electromagnetic split-step fast Fourier transform terrain parabolic equation propagation model within a Bayesian inversion framework. In contrast to the global optimization algorithm, the Bayesian–MCMC can obtain not only the approximate solutions, but also the probability distributions of the solutions, that is, uncertainty analyses of solutions. The Bayesian–MCMC algorithm is implemented on the simulation radar sea-clutter data and the real radar sea-clutter data. Reference data are assumed to be simulation data and refractivity profiles are obtained using a helicopter. The inversion algorithm is assessed (i) by comparing the estimated refractivity profiles from the assumed simulation and the helicopter sounding data; (ii) the one-dimensional (1D) and two-dimensional (2D) posterior probability distribution of solutions.

Keywords: refractivity from clutter, terrain parabolic equation propagation model, Bayesian–Markov chain Monte Carlo, uncertainty analysis

PACS: 93.85.Ly, 41.20.Jb **DOI:** 10.1088/1674-1056/22/2/029302

1. Introduction

Surface-based ducts appear about 15% of the time worldwide, 25% of the time off Southern California Coast, and about 50% of the time in the Persian Gulf. While surface-based ducts are less common than evaporation ducts, their effects are frequently more dramatic.[1] A duct is an anomalous atmospheric condition, and it can directly affect the performance of various radio systems due to the anomalous propagations of electromagnetic waves.[2] Ducts result in various anomalies such as change in the maximum operational radar range and the creation of radar holes where radar cannot work. Hence, it is necessary to understand the effects of the environment on radio systems/radar system performance.

Traditionally, atmospheric ducts can be measured using rocketsondes, radiosondes, microwave refractometers, ground-based global positioning system (GPS), and numerical weather models. However, these techniques are costly and cannot provide real-time duct parameters. Estimation of atmospheric ducts from radar clutter can provide near-real-time parameters of ducts without using additional hardware or extra meteorological measurements. Researchers have performed many theoretical and experimental studies. An experiment (called Wallops98) was carried out to estimate the parameters of atmospheric ducts from radar clutter, whose results show the feasibility and efficiency of the RFC technique. Inferring refractivity parameters from radar clutter is a complicated inverse problem, because the relationship between refractivity value and radar sea clutter is clearly nonlinear. A global optimization algorithm might be a good choice to acquire approximate solutions. Tabrikian *et al*.[3] proposed a maximum a posteriori (MAP) approach to jointly estimating the refractivity and the spatially varying backscatter cross section. Gerstoft, Rogers *et al*.,[4] Barrios,[5] and Gerstoft, Hodgkiss *et al*.[6] proposed the usage of a genetic algorithm (GA) to estimate the refractivity profile.

Bayesian inversion is a likelihood-based algorithm, and when combined with a powerful sampling algorithm such as Markov Chain Monte Carlo (MCMC) it can be an effective tool in estimating the uncertainties in nonlinear inversion problems, such as the electromagnetic refractivity uncertainties in nonlinear inversion problems, and the electromagnetic refractivity from clutter inversion.[7–9] Bayesian–MCMC can obtain variance and the marginal posterior probability distribution of each estimated parameter. Bayesian–MCMC can provide unbiased sampling of the posterior probability density (PPD), unlike global optimizers such as the genetic algorithm, which usually oversamples the peaks of the PPD and brings in a bias.

*Project supported by the National Natural Science Foundation of China (Grant No. 41105013), the National Natural Science Foundation of Jiangsu Province, China (Grant No. BK2011122), the Open Issue Foundation of Key Laboratory of Meteorological Disaster of Ministry of Education, China (Grant No. KLME1109), and the City Meteorological Scientific Research Fund, China (Grant No. IUMKY&UMRF201111).

†Corresponding author. E-mail: 19994035@sina.com

© 2013 Chinese Physical Society and IOP Publishing Ltd

2. Forward model

2.1. Environmental and propagation model

The five-parameter refractivity model was proposed by Gerstoft *et al*.[4] of the Naval Force Physics Laboratory in California, which can be described as

$$\boldsymbol{m} = (\delta, c_1, z_\mathrm{b}, z_\mathrm{thick}, M_\mathrm{d})^\mathrm{T}. \tag{1}$$

Here, δ is the evaporation duct height, c_1 is the slope in the mixed layer, z_b is the trapping-layer base height, z_thick is the thickness of the inversion layer, and M_d is M deficit of the inversion layer. The value of modified refractivity as a function of height z is given by

$$M(z) = M_0 + \begin{cases} M_1 + c_0\left(z - \delta\log\dfrac{z}{z_0}\right), & \text{for } z < z_\mathrm{d}, \\ c_1 z, & \text{for } z_\mathrm{d} < z < z_\mathrm{b}, \\ c_1 z_\mathrm{b} - M_\mathrm{d}\dfrac{z - z_\mathrm{b}}{z_\mathrm{thick}}, & \text{for } z_\mathrm{b} < z < z_\mathrm{t}, \\ c_1 z_\mathrm{b} - M_\mathrm{d} + c_2(z - z_\mathrm{t}), & \text{for } z_\mathrm{t} < z. \end{cases} \tag{2}$$

In practical implementations, prior information might be available from a variety of sources (e.g., numerical weather prediction models, atmospheric soundings, etc.), thereby improving the qualities of the inverse problem solutions. Details about the boundary of refractivity parameters can be seen from Ref. [10]. The most commonly used approach to modeling the wave propagation in the troposphere is the Fourier split-step solution to the parabolic equation. This numerical solver is a forward model with the ability to handle vertical and horizontal inhomogeneities in complicated environments.

2.2. Radar model

The received power P_c from radar sea clutter can be calculated from[10]

$$P_\mathrm{c} = \frac{4\pi P_\mathrm{t} G_\mathrm{t} G_\mathrm{r} A_\mathrm{c} \sigma^0}{L_\mathrm{loss}^2 \lambda^2}. \tag{3}$$

Here, P_t is the transmitted power, G_t is the transmitted antenna gain, G_r is the receiving antenna gain, λ is the wavelength, A_c is the illuminated area, and σ^0 is the normalized radar cross section of sea clutter. At low grazing angles, A_c is a linear function of range r, so Eq. (3) can be rewritten as

$$P_\mathrm{c} = \frac{C\sigma^0 r}{L_\mathrm{loss}^2}. \tag{4}$$

Here, C covers all of the constant terms in Eq. (3). Letting the symbols P_c, C, σ^0, and L be all in units of dB, the received signal power from the clutter can be modeled as

$$P_\mathrm{c} = -2L_\mathrm{loss} + 10\log_{10}(r) + \sigma^0 + C. \tag{5}$$

Here, some stochastic variations in range as a Markov process are simulated as noises, σ^0 is the radar cross section (RCS) of the sea surface, C is a constant that includes wavelength, transmitter power, antenna gain, etc., and $\sigma^0 \propto$ grazing angle φ^0 in the duct height estimation algorithm generated better results. This model is chosen here.

2.3. The terrain parabolic equation model (TPEM)

In smooth, perfectly conducting surface and horizontal polarization conditions, tropospheric radiowave propagation over the sea in the presence of range-dependent refractivity is presented as the TPEM.[11] It can be described as such an initial value problem

$$\partial_z^2 u + 2\mathrm{i}k_0\partial_x u + k_0^2(\boldsymbol{m}^2 - 1)u = 0, \tag{6a}$$

$$u(x,0) = 0, \tag{6b}$$

$$u(0,z) = \phi(z). \tag{6c}$$

Here, 0 is the free space wave number, $\boldsymbol{m}(x,z)$ is the modified index of refraction, $\boldsymbol{m}(x,z)$ is defined by $m = n + z/a_\mathrm{e}$ that takes into account the Earth's curvature, n is the index of refraction, and a_e is the radius of the Earth. $u(x,0) = 0$ represents the boundary condition at $z = 0$, and $u(0,z) = \varphi(z)$ gives the initial field in the source range.

For range x_k and height z, if $u(x_k,z)$ is the electromagnetic field, then the field in range x_{k+1} and at height z, denoted by $u(x_{k+1},z)$, can be obtained by the split-step Fourier solution, and expressed as

$$u(x_{k+1},z) = \exp\left(\mathrm{i}\frac{k_0}{2}\left(m^2 - 1\right)\delta x\right) F^{-1} \times \left\{\exp\left(-\mathrm{i}\frac{p^2\delta x}{2k_0}\right) F\left[u(x_k,z)\right]\right\}. \tag{7}$$

Here, $F[\cdot]$ and $F^{-1}[\cdot]$ are the Fourier transform and inverse Fourier transform, respectively, δx is the range increment, denoted by $\delta x = x_{k+1} - x_k$. p is the transform variable referred to as the vertical wave number or the spatial frequency.

3. Bayesian–MCMC method

3.1. Bayesian–MCMC theory

To address the uncertainties in the refractivity parameter estimates, the basic quantities such as mean, variance, and marginal posterior probability distribution of each estimated parameter need to be determined. These parameters can be computed by taking multi-dimensional integrals of the PPD, which can be accomplished by an MCMC sampling of the PPD. A split-step FFT parabolic equation code is used in the MCMC sampler as its forward propagation model.

The probability function $p(\boldsymbol{m}|\boldsymbol{d})$ can be defined as the probability of the model $\boldsymbol{m}$, and given the observation data $\boldsymbol{d}$. The prior $p(\boldsymbol{m})$ represents prior knowledge of the environmental parameters $\boldsymbol{m}$ before the experimental observation data. So, it is independent of the experimental results. $p(\boldsymbol{d})$ is the normalizing factor for $p(\boldsymbol{m}|\boldsymbol{d})$ and it is independent of the parameter vector $\boldsymbol{m}$. A flat prior assumption can be reduced to

$$p(\boldsymbol{m}|\boldsymbol{d}) \propto L(\boldsymbol{m}). \tag{8}$$

Here, a zero-mean Gaussian-distributed error is assumed, and $L(\boldsymbol{m})$ is a likelihood function and can be rewritten as

$$L(\boldsymbol{m}) = (2\pi)^{-N_R/2} \cdot |\boldsymbol{C_d}|^{-1/2} \times \exp\left[-\frac{(\boldsymbol{d}-e(\boldsymbol{m}))^T \boldsymbol{C_d^{-1}} (\boldsymbol{d}-e(\boldsymbol{m}))}{2}\right], \quad (9)$$

where $\boldsymbol{d}$ is the radar clutter observation data vector, $e(\boldsymbol{m})$ is the forward model function value, $\boldsymbol{C_d}$ is the data covariance matrix, N_R is the number of used range points. On this occasion, $\boldsymbol{C_d} = \nu \boldsymbol{I}$, with ν being the variance and $\boldsymbol{I}$ the identity matrix. Error function $\phi(\boldsymbol{m})$ is defined as

$$\phi(\boldsymbol{m}) = |\boldsymbol{d} - e(\boldsymbol{m})|^2 = \sum_{i=1}^{N_R} |d_i - e(m_i)|^2. \quad (10)$$

The likelihood function $L(\boldsymbol{m})$ can be simplified as

$$L(\boldsymbol{m}) = (2\pi\nu)^{-N_R/2} \cdot \exp\left[-\frac{\phi(\boldsymbol{m})}{2\nu}\right]. \quad (11)$$

Therefore, the posterior probability density $p(\boldsymbol{m}|\boldsymbol{d})$ can be rewritten as

$$p(\boldsymbol{m}|\boldsymbol{d}) \propto \exp\left[-\frac{\phi(\boldsymbol{m})}{2\nu}\right]. \quad (12)$$

3.2. Implementation of the Bayesian–MCMC method

The vertical structure of the refractivity environment is modeled using five parameters. Calculating the probabilities of all possible combinations in a predetermined grid is known as an exhaustive search, depending on the forward modeling computation speed. It becomes impractical because classic Metropolis/Gibbs sampling is impractical due to too much computation. So, there is a need to have an effective technique that can reduce computation. There are two main drawbacks of the Bayesian–MCMC method which lead to reducing the computation speed. The first drawback is related to the distance between the starting point and the high probability region. The second drawback is the correlation effect of refractivity parameters, which leads to the difficulty in sampling the highly correlated PPD regions.

The first drawback can be solved by the initial sampling technique. The classical MCMC method should be improved to include an initialization phase, which is referred as the "burn-in" phase. In most cases, the burn-in section is a global optimizer, such as the genetic algorithm (GA) or the fast cooling simulated annealing (SA) algorithm.

The second drawback can be solved by using a coordinate rotation technique. The classical MCMC method samples only in the directions parallel to parameter axes in the vertical and horizontal directions; it is hard to sample highly correlated PPD but it can be done with a much smaller number of samples in an uncorrelated region. A new set of uncorrelated parameter space, which is determined by applying an orthogonal coordinate transformation, rather than the correlated parameter space, is used to solve the above problem and the orthogonal coordinate transformation diagonalizes the model covariance matrix. The model covariance matrix is found by using samples drawn from the PPD after the burn-in phase. Due to its fast converging nature, only a small number of MCMC samples are needed to find the model covariance matrix.

The final sampling phase consists simply of two parallel-running, independent samplers (Metropolis or Gibbs) in the rotation space, sampling the same PPD. The Kolmogorov–Smirnov (KS) statistic function of the marginal posterior distribution is used as a convergence criterion. When the convergence criterion is met, these two independent sets are combined into a final set, whose error is twice as large, which is expected to be less than the error between the true distribution and the estimated one. The whole inversion flow chart of the Bayesian–MCMC is shown in Fig. 1.

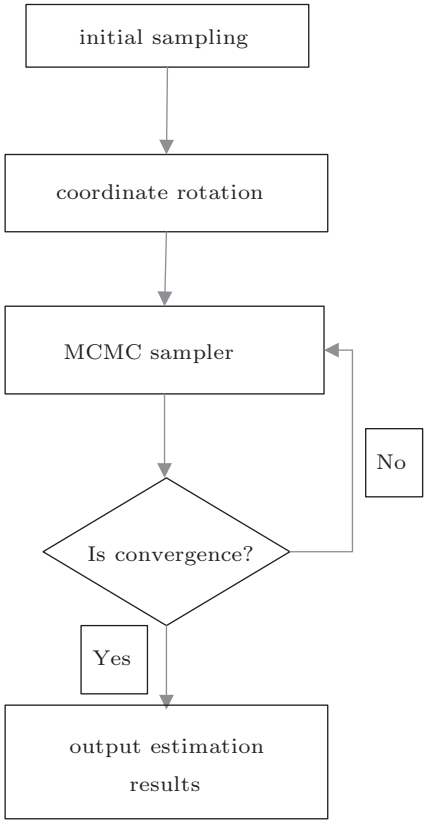


Fig. 1. Flow chart of the Bayesian–MCMC method.

4. Inversion of simulation radar sea-clutter data

In order to test the Bayesian–MCMC algorithm, a comparison with the true distribution is necessary. The estimated parameters are chosen to be δ, c_1, z_b, z_{thick}, and M_d, and they are described as m_1, m_2, m_3, m_4, and m_5 in Fig. 2. The synthetic data are generated by the TPEM at a frequency of 8.0 GHz, antenna gain of 30 dB, beamwidth of 1.5°, and antenna height of 15.0 m. The distributions of 1D estimated parameters are given in Fig. 2

The final sampling phase simply is composed of two independent, parallel-running Gibbs samplers, each of which performs effective sampling 41093 times. So, two samplers perform the effective sampling data 82186 times in total. The effective sampling data are described as a histogram in Fig. 2. Markov chain I is the first Markov chain sampling data; Markov chain II is the second Markov chain sampling data; Markov chain I+II is the total sampling data; the solid line represents the true value.

It can be seen from Fig. 2 that the sampling result is close to the true value. The estimation accuracy from high to low is ordered as $\delta(m_1)$, $z_{\rm thick}(m_3)$, $z_{\rm b}(m_4)$, $M_{\rm d}(m_5)$, $c_1(m_2)$. The estimation results are in accordance with the sensitivity research results of refractivity parameters.[12,13]

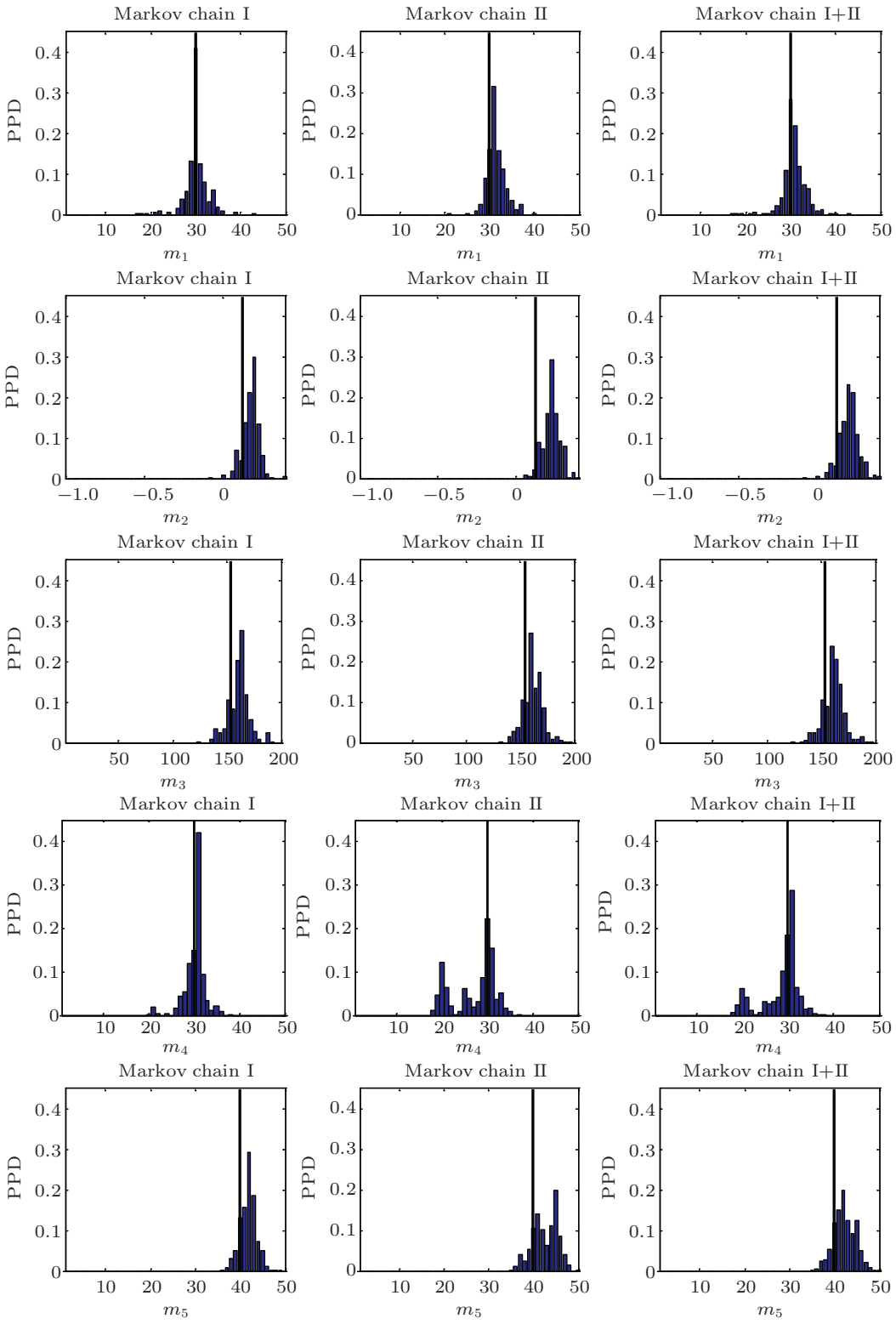


Fig. 2. (color online) Distributions of 1D estimated parameters.

5. Inversion of Wallops98 data

The ducting event occurred on April 1998 on Wallops Island, and radar clutter data were obtained using the space range radar, which is known as SPANDAR. Meteorological soundings were obtained by an instrumented helicopter which flew in and out on the 150-deg radial from a point 4-km due east of the SPANDAR. The distributions of 1D estimated parameters are given in Fig. 3; marginal and 2D posterior distributions obtained by the Gibbs sampler are given in Fig. 4; a comparison between the refractivity parameters from the helicopter soundings and those estimated is given in Fig. 5.

Posterior probability distribution maps of the $\boldsymbol{m} = (z_b, M_d, z_{\text{thick}}, c_1, \delta)^{\text{T}}$ can be seen in Fig. 3, where the maps from top to bottom are for z_{b} (base height), M_{d} (M-deficit), z_{thick} (thickness), c_1 (slope mixer layer), δ (evaporation thickness). The posterior probability of parameters in sampling regions can be seen from the Y-axis value, indicating that the posterior probability of c_1 concentrates in a $(-0.4, -0.05)$ region and δ in a $(20, 35)$ region, other parameters' posterior probabilities are equally distributed in the whole sampling region.

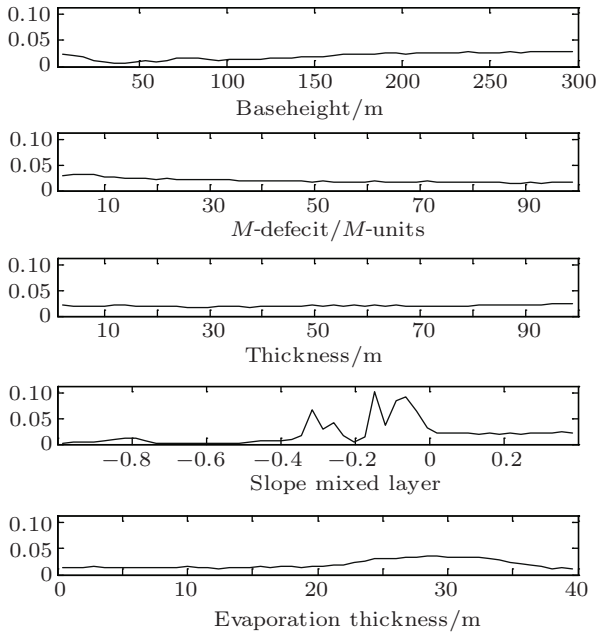


Fig. 3. Distributions of 1D estimated parameters for Wallops98 data.

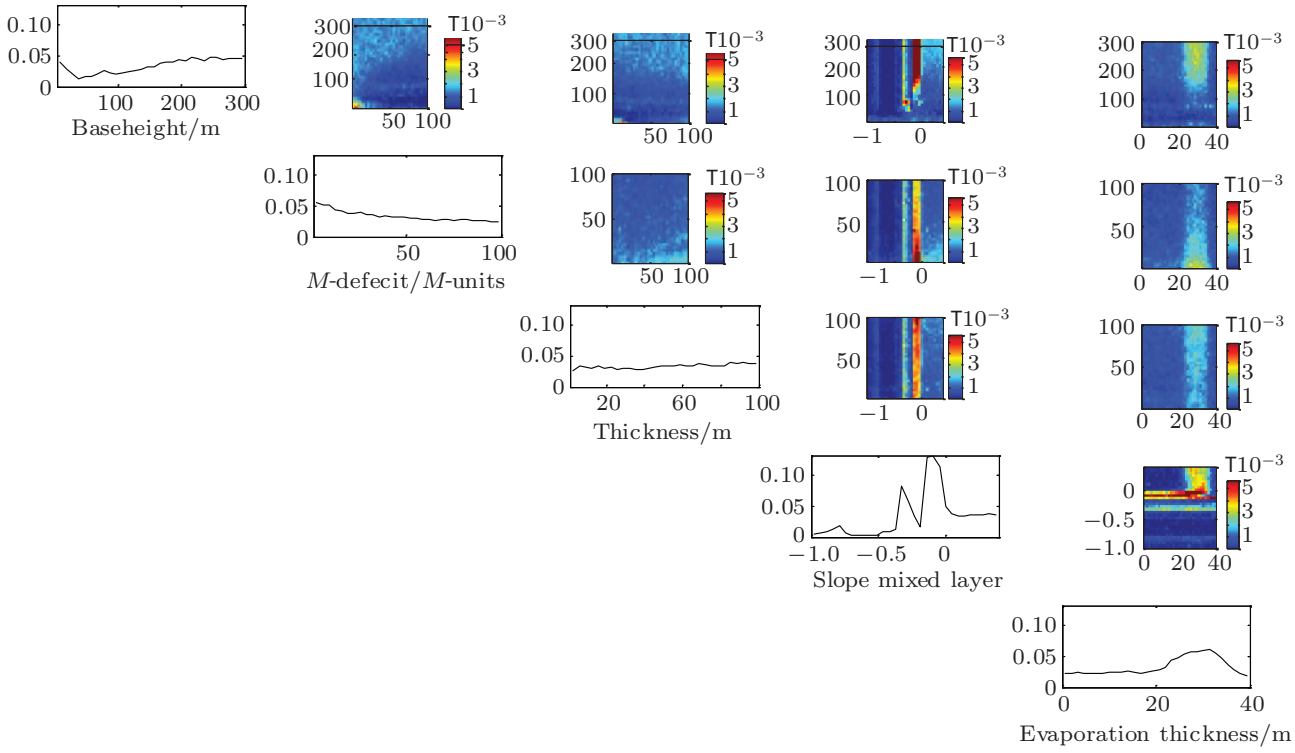


Fig. 4. (color online) Distributions of 2D estimated parameters for Wallops98 data.

The 2D posterior probability distribution maps of the $\boldsymbol{m} = (z_b, M_d, z_{\text{thick}}, c_1, \delta)^{\text{T}}$ can be seen in Figs. 4. The 2D posterior probabilities of parameters in sampling regions can be seen from the gray map value. The light gray value shows high posterior probability distribution, the dark gray value indicates low posterior probability distribution, and the reference 2D posterior probability value can be seen in the gray bar. It can be seen that 2D posterior probabilities concentrate in the c_1 and the δ region, and the 2D posterior probabilities of other parameters are equally distributed in the whole sampling

region.

Figure 5 summarizes the inversion and assessment of the inversion results from Bayesian–MCMC method. First, the radar sea clutter $\boldsymbol{P}_{\rm c}^{\rm obs}$ at an azimuth angle of 150° and in a range of 10 km–60 km is shown as a black solid line in Fig. 5(a). Three clutter-return contrasts are seen from 10 km to 60 km. The Bayesian–MCMC estimation result is shown as dash-dotted line, and for reference, the modeled clutter returns from the helicopter profiles are denoted as dotted line. Figure 5(b) shows the estimated refractivity profile (dash-dotted line) together with the helicopter refractivity profile (solid line). Because this is an undetermined problem, the inversion result might not correspond to the true profile. Figures 5(c) and 5(d) display the modeled propagation loss for the sampling environment and the helicopter profile, respectively. The difference between these two (bottom plot) gives an indication of how well the inverted profile is able to predict the propagation loss (Fig. 5(e)). It can be seen that the Bayesian–MCMC inversion result is close to the true profile, and better than that obtained from the global optimization algorithm (GA), because the difference between these two figures (i.e., Figs. 5(c) and 5(d)) is very small, and the difference between regions is mostly less than 10 dB.

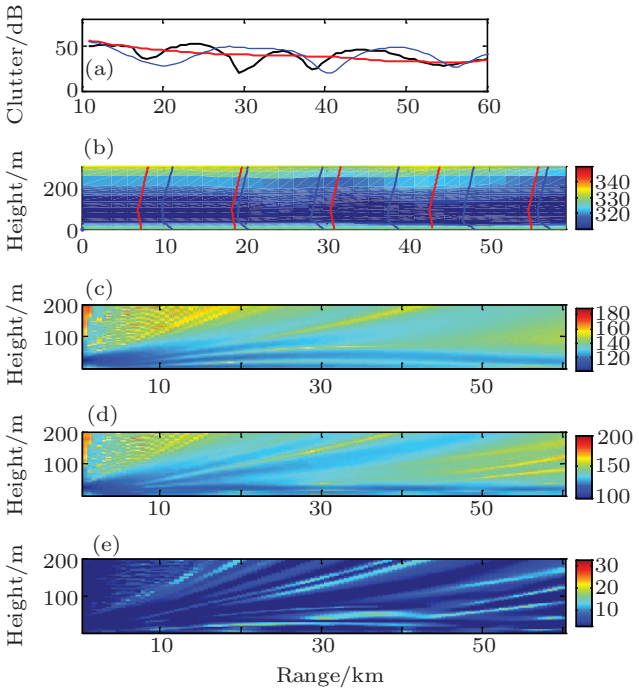


Fig. 5. (color online) Inversion results based on the Wallops98 data using the Bayesian–MCMC method, showing (a) the clutter return (in dB) as observed by the radar data (dotted), the modeled return using the retrieval profile (dash dotted), and modeled return from the observed profile (solid line); (b) observed profiles measured from helicopter (solid line) and to retrieval profiles (dash dotted); (c) coverage diagram (dB) corresponding the inverted profiles; (d) coverage diagram (dB) based on helicopter profiles; (e) difference (dB) between coverage diagrams Figs. (5c) and (5d).

6. Conclusion

An uncertain estimation refractivity from radar sea clutter is described using the Bayesian–MCMC method. A five-parameter range-independent parameterization is introduced and the Bayesian–MCMC algorithm is employed to handle the large search space.[14–17] The parameterization and search bounds that are used can easily accommodate refractivity profiles found in other regions of the world.[18] The Bayesian–MCMC method can obtain full n-dimensional posterior probability distributions for the unknown parameters and the maximum likelihood solution itself. Comparisons with global optimization algorithm (GA) results show that MCMC samplers require more samples than the classical global optimizer but are better in estimating probability distributions. The Bayesian–MCMC method can obtain more accurate inversion results than the global optimizer, but it needs a relatively large number of forward model runs. The main advantage of the Bayesian–MCMC method is that it can obtain the probability distributions of solutions, that is, uncertainty analyses of solutions.

Acknowledgement

The authors would like to thank professors P Gerstoft and C Yardim of the Marine Physical Laboratory, University of California, San Diego, for providing SPANDAR data.

References

[1] Rogers L T, Hattan C P and Stapleton J K 2000 *Radio Sci.* **35** 955
[2] Wei M, Qin X, Wang X H and Jiang W M 2007 *Trans. Atmos. Sci.* **30** 736 (in Chinese)
[3] Tabrikian J and Krolik J K 1999 *IEEE Trans. Antennas Propag.* **47** 1727
[4] Gersoft P, Rogers L T, Krolik J K and Hodgkiss W S 2003 *Radio Sci.* **38** 2640
[5] Barrios A 2004 *Radio Sci.* **39** 2930
[6] Gerstoft P, Hodgkiss W S, Rogers L T and Jablecki M 2004 *Radio Sci.* **39** 3077
[7] Yardim C, Gerstoft P and Hodgkiss W S 2006 *IEEE Trans. Antennas Propag.* **54** 1318
[8] Vasudevan S, Anderson H R, Kraut S, Gerstoft P, Rogers L T and Krolik J L 2007 *Radio Sci.* **42** 3423
[9] Yardim C, Gerstoft P and Hodgkiss W S 2007 *Radio Sci.* **42** 3561
[10] Sheng Z and Fang H X 2012 *Chin. Phys.* B **21** 029301
[11] Yardim C, Gerstoft P and Hodgkiss W S 2008 *IEEE Trans. Antennas Propag.* **56** 1058
[12] Douvenot R, Fabbro V, Gerstoft P, Bourlier C and Saillard J 2008 *Radio Sci.* **43** 3842
[13] Yardim C, Gerstoft P and Hodgkiss W S 2009 *Radio Sci.* **44** 3897
[14] Sheng Z and Huang S X 2009 *Acta Phys. Sin.* **58** 4328 (in Chinese)
[15] Sheng Z and Huang S X 2010 *Acta Phys. Sin.* **59** 1734 (in Chinese)
[16] Sheng Z and Huang S X 2010 *Acta Phys. Sin.* **59** 3912 (in Chinese)
[17] Sheng Z 2011 *Acta Phys. Sin.* **60** 119301 (in Chinese)
[18] Guo P, Kuo Y H, Sokolovskiy S V and Lenschow D H 2011 *J. Atmos. Sci.* **68** 1703